Original Article

Machine-Learning Identifies a Strategy for Differentiation Therapy in Solid Tumors

Authors: Saptarshi Sinha, Ph.D[1], Joshua Alcantara, B.S.[1, 2], Kevin Perry, B.S.[1, 2], Vanessa Castillo, B.S.[1], Celia R. Espinoza, Ph.D. [1], Sahar Taheri, B.S.[3], Eleadah Vidales, B.S.[1, 2], Courtney Tindle, M.S.[1, 2], Adel Adel, B.S.[1], Siamak Amirfakhri, D.V.M, Ph.D.[5], Joseph R. Sawires, B.S.[6], Jerry Yang, Ph.D. [6], Michael Bouvet, M.D.[5,7], Debashis Sahoo, Ph.D. [3,4,7] and Pradipta Ghosh, M.D.[1,2,7,8‡]

Affiliations:

[1]Department of Cellular and Molecular Medicine, School of Medicine, University of California San Diego, La Jolla, CA 92093.

[2]HUMANOID™ Center of Research Excellence (CoRE), University of California San Diego, La Jolla, CA 92093.

[3]Department of Computer Science and Engineering, Jacob's School of Engineering, University of California San Diego, CA 92093.

[4]Department of Paediatrics, School of Medicine, University of California San Diego, La Jolla, CA 92093.

[5]Department of Surgery, University of California San Diego, San Diego, CA 92093, USA; Department of Surgery, VA San Diego Healthcare System, San Diego, CA, USA.

[6]Department of Chemistry and Biochemistry, University of California San Diego, San Diego, CA, 92093, USA.

[7]Moores Cancer Center, University of California San Diego, San Diego, CA, 92093, USA.

[8]Department of Medicine, University of California San Diego, San Diego, CA, 92093, USA.

‡**Corresponding author and Lead Contact**: Pradipta Ghosh, M.D.; Professor, Departments of Medicine and Cellular and Molecular Medicine, University of California San Diego; 9500 Gilman Drive (MC 0651), George E. Palade Building, Rm 232, 239; La Jolla, CA 92093. Phone: 858-822-7633. Email: prghosh@ucsd.edu.

Abstract

Background: Although differentiation therapy can 'cure' some hematologic malignancies, its curative potential remains unrealized in solid tumors. This is because conventional computational approaches succumb to the thunderous noise of inter-/intratumoral heterogeneity. Using colorectal cancers (CRCs) as an example, here we outline a machine learning(ML)-based approach to track, differentiate, and selectively target cancer stem cells (CSCs).

Methods: A transcriptomic network was built and validated using healthy colon and CRC tissues in diverse gene expression datasets (~5,000 human and >300 mouse samples). Therapeutic targets and perturbation strategies were prioritized using ML, with the goal of reinstating the expression of a transcriptional identifier of the differentiated colonocyte, CDX2, whose loss in poorly differentiated (CSC-enriched) CRCs doubles the risk of relapse/death. The top candidate target was then engaged with a clinical-grade drug and tested on 3 models: CRC lines *in vitro*, xenografts in mice, and in a prospective cohort of healthy (n = 3) and CRC (n = 23) patient-derived organoids (PDOs).

Results: The drug shifts the network predictably, induces *CDX2* and crypt differentiation, and shows cytotoxicity in all 3 models, with a high degree of selectivity towards all *CDX2*-negative cell lines, xenotransplants, and PDOs. The potential for effective pairing of therapeutic efficacy (IC50) and biomarker (*CDX2*-low state) is confirmed in PDOs using multivariate analyses. A 50-gene signature of therapeutic response is derived and tested on 9 independent cohorts (~1700 CRCs), revealing the impact of *CDX2*-reinstatement therapy could translate into a ~50% reduction in the risk of mortality/recurrence.

Conclusions: Findings not only validate the precision of the ML approach in targeting CSCs, and objectively assess its impact on clinical outcome, but also exemplify the use of ML in yielding clinical directive information for enhancing personalized medicine.

Introduction

Poor differentiation (increased stemness) is a hallmark of cancers; differentiation therapy that can target the cancer stem cells is expected to improve outcomes. A poster child of differentiation therapy is all-trans-retinoic acid (ATRA), which has achieved a 'cure' for the otherwise fatal acute promyelocytic leukemia (APML)[1-10]. Although differentiation therapy with a few other agents has been achieved in leukemia[11,12], it is yet to be realized in carcinomas. One of the reasons often cited for such failure is the thunderous intra- and inter-tumoral heterogeneity that limits our ability to track the identity the few cancer stem cells[13] (CSCs) that lie within the tumor. To look past such heterogeneity, computational algorithms have emerged as popular approaches to sort through 'big data' (such as transcriptomics), build networks, understand complex human diseases, and even prioritize targets. For example, mapping the network of robust relationships between genes has been a popular tool for understanding human diseases[14-19]. Pair-wise gene connections are usually established by performing correlation[20-25], mutual information[17] or other symmetric computational frameworks such as linear regression[26], dimension reduction[27], and clustering[28,29]. These methods often succumb to the heterogeneity in the real-world. More recently, a network transcriptomics-based approach, in which gene clusters relate to each other via directed edges of Boolean invariant relationships[30,31], has been successfully used to extract insights from heterogeneous big data and create maps of evolving cellular states along any disease continuum. This methodology has been used to identify translationally relevant cell states with high degrees of precision in diverse contexts and tissues[32-45]; most recently it has been used to identify a first-in-class therapeutic target to protect the vulnerable gut barrier in inflammatory bowel disease[30].

As for the therapeutic goal of the network, we set it as reinstatement of CDX2 which is a nuclear homeobox transcription factor and a tumor suppressor that belongs to the caudal-related family of CDX homeobox genes[46-49]. In 2016, an unbiased search (using the same Boolean logic approach[50,51]) looking for a biomarker of tumor stemness/differentiation status identified CDX2 as the statistically top ranked candidate biomarker of mature colon epithelial tissues, and by that token, of well-differentiated tumors [52]. The study predicted *CDX2* as the top developmentally regulated pro-differentiation candidate gene whose expression in colorectal cancer (CRCs) was inversely related to the "activated leukocyte cell adhesion molecule" (*ALCAM*/CD166); the latter is a marker of stem-like colon epithelial cells at the bottom of colon crypts[53,54] and on human colon cancer cells with high tumorigenic capacity in mouse xenograft models[55]. Validation studies using immunohistochemistry (IHC) showed that compared to patients with CDX2-pos tumors, those with a loss of CDX2 (accounting for approximately 9% of patients) had lower disease-free survival (DFS) and benefited from an adjuvant chemotherapy, even in stage II CRC.

Numerous groups have since reproduced the prognostic claims [56-69]. Thirty-two independent studies, involving >13,000 unique subjects, most that used IHC and one that used IHC in combination with quantitative mass spectrometry [70], have determined that CDX2-neg CRCs are associated with lower overall survival (OS) and DFS independent of ethnicity, DNA mismatch repair (MMR) status or stage [52,65,69,71] [**Figure 1**-*Step 1*]. Absence of CDX2 in tumors is associated with several adverse prognostic features, such as poor differentiation, advanced stage, vascular invasion, right-sided location, CpG island methylator phenotype (CIMP), and *BRAF* mutation [71-73]. Presence of CDX2 lowers the risk of death and recurrence by 50% and

90 52%, respectively[69]; this finding is more pronounced in stage II and III CRCs, with up to 70% reduction in the
91 risk of death. These findings drove consensus that pharmacologic reinstatement of CDX2 in CRCs is a
92 clinically important therapeutic goal [see **Figure 1**-*Step 1*], one that is also challenging because promising
93 candidates have not emerged.
94
95 Here we adopted the same Boolean-logic-based network transcriptomic approach[50,51] to screen for
96 therapeutic targets that can induce CDX2 and promote tumor differentiation.
97

Methods: Detailed computational and experimental methods are presented in ***Supplementary Materials*** and mentioned briefly here.

Bioinformatics analysis of gene-expression array databases. A complete catalogue of all the NCBI-GEO sample number identifiers (GSEIDs) of individual gene-expression array experiments used for model training and validation are provided (**Supplemental Information 1**).

Patient derived organoids. To enhance reproducibility and rigor, all CRC PDOs used in this work were acquired from the American Type Culture Collection (ATCC), which acquired these from diverse clinical sources [The Human Cancer Models Initiative (HCMI) US National Cancer Institute (NCI), Cancer Research UK (CRUK), the Wellcome Sanger Institute (WSI), and the foundation Hubrecht Organoid Technology (HUB)]. Relevant demographic, clinical and genetic information is provided (**Supplemental Information 3**).

Statistical tests. Optimal cut-off values of gene expression levels are derived using a threshold defined by *StepMiner* algorithm in the individual dataset[74]. Gene signature is used to classify sample categories and the performance of the multi-class classification is measured by ROC-AUC (receiver operating characteristics area under the curve) values. Standard t-tests were performed using python scipy.stats.ttest_ind package (version 0.19.0) with Welch's two sample t-test (unpaired, unequal variance (equal_var = False), and unequal sample size) parameters. Multiple hypothesis correction were performed by adjusting p-values with statsmodels.stats.multitest.multipletests (fdr_bh: Benjamini/Hochberg principles). Differential expression analysis was performed in DESeq2 in R (version 1.16.1). Kaplan–Meier analysis and determination of statistical significance by Log Rank test was performed using GraphPad Prism 9.1. Violin and Bubble plots are created using python seaborn package version 0.12. BooleanNet algorithm is used to statistically determine Boolean Implication relationships between genes (statistic > 3 and error-rate < 0.1). The source code for Boolean analysis framework is https://github.com/sinha7290/Prodiff[32]. The best estimate of effect size (ratio between the difference in mean and standard deviation) is 2.5 in PDO and 1.0 in animal experiment for CDX2 induction using PRKAB1-agonist. The sample size in each group of at least 4 PDOs and 17 animals should suffice (α = 0.05 and power = 0.80).

Study Design. The study was designed by the first and last author. All authors contributed to the gathering, analysis, and interpretation of the data. The first draft of the manuscript was written by the first and last author and was subsequently edited based on comments from all authors.

Ethics statement. This study was carried out in strict accordance with the recommendations in the Guide for the Care and Use of Laboratory Animals of the National Institutes of Health. All animal studies were approved by the San Diego Veterans Administration Medical Center Institutional Animal Care and Use Committee (protocol A17-020; PI Bouvet). All colorectal cancer PDOs were obtained from the American Type Culture Collection (ATCC). The latter is a nonprofit, global biological resource centre and a distributor of organoid models curated as part of Human Cancer Models Initiative (HCMI) for enhancing reproducibility. Deidentified case-associated data, including that of molecular characterization of the models, the tissues from which they were derived were used here, whereas available harmonized data are accessible through NCI's Genomic Data Commons. All healthy colon PDOs were obtained from individuals presenting for routine colonoscopy as part of colon cancer screening at UC San Diego, with their informed consent to participate in a study protocol approved by an Institutional Review Board (IRB; protocol #190105; PI Ghosh).

Role of funders

Funders of the study had no role in study design, data collection, data analyses, interpretation, or writing of report.

Results

A network-rationalized approach

We used a machine learning-based computational platform, Boolean Network Explorer (*BoNE*)[30], and *CDX2* as a 'seed' gene to create a model of progressive gene regulatory events that occur during differentiation in the colon (**Figure 1**-*Step 2;* **Figure S1A-B**). The model was trained on a pooled heterogeneous dataset that included maximum possible diversity (1662 CRCs, 68 adenomas and 170 normal tissues) (**Figure S1C-D**). Statistical learning on the *CDX2*-proximal immediate gene clusters (clusters #2 and #3, **Figure S1D**) helped statistically rank 5 genes as top targets (**Figure 1**-*Step 2;* **Figure S1E**). By virtue of how these genes relate to *CDX2* within the network, upregulation of any of these 5 genes (presumably via target/pathway agonists) is predicted to also upregulate *CDX2*. Validation studies on an additional 2,937 human (**Figure S1F**) and 318 mouse (**Figure S2**) colon samples showed that these 5 genes remain relevant across species and diverse cohorts.

In search of potent and specific drugs to modulate the 5 targets, we searched the PDB [Protein Data Bank; https://www.rcsb.org] for structure resolved selective agonistic modulators and found 25 molecules/structures for PRKAB1, but none for the remaining targets. To determine the most clinically advanced candidate, the PDB-derived hits were cross-searched through the Clinical Trials.gov portal, which led to the identification of a clinical-grade drug, PF-06409577 (henceforth, PF). Although lacking clinical indication at present, the drug was deemed safe in a randomized, double-blind, placebo-controlled Phase I trial [*ClinicalTrials.gov* ID: NCT02286882]. Furthermore, PF was recently shown to demonstrate target specificity and the ability to upregulate the *PRKAB1* transcript and the translated protein in the colonic epithelium ex-vivo and mouse colon in vivo[30].

The network model predicted that the agonism of the protein that is translated by the *PRKAB1* gene, i.e., Protein Kinase AMP-activated Non-Catalytic Subunit Beta-1 will-- (i) upregulate *PRKAB1* expression and, by virtue of their "*equivalent*" relationship, also upregulate the other genes that co-cluster with it (**Figure S1D**); (ii) upregulate *CDX2* and the *CDX2*-proximal gene clusters (#2 and #3) by virtue of "hi=>hi" relationship (**Figure S1D**); and (iii) downregulate stemness genes by virtue of "hi=>lo" relationship (*CCDC88A* and others in C#9; **Figure S1D**). Notably, *PRKAB1* has a universally conserved relationship with *CDX2*, across diverse human and mouse CRC datasets, including early onset CRCs (**Figure S2A-D**). That PRKAB1 (but not the other β-subunit, PRKAB2) is strongly expressed in the GI tract[30] and that PRKAB1-agonists trigger cell polarity in the gut epithelium[75-78], served as additional justifications for its rationalized selection as target.

For target validation, we prioritized three models, based on their *CDX2*-low (target tumor type) and high (expected to be negative control) status. Alongside the traditional readouts of anti-cancer effects, a set of additional end points were *a priori* formulated as metrics of success; therapeutic goal was set such that all three models must pass all three end points (see **Figure 1**-*Step 3*). Prior attempts that successfully induced *CDX2* temporarily[79], but ultimately failed to emerge as differentiation therapy, had mixed impact on these metrics of success (**Figure S3**). Finally, to track successful *CDX2*-reinstatement and assess its impact on survival, a 50-gene signature of therapeutic response is derived and tested on numerous independent cohorts (see **Figure 1**-*Step 4*).

Target validation on CRC cell lines and xenograft models

178 Next, we prioritized two poorly differentiated CRC cell lines (HCT116 and Sw480 cells; both exhibited the
179 lowest levels of *CDX2* transcripts among a panel of 26 sequenced CRC cell lines that were profiled by
180 microarrays; GSE10843) as the optimal models for hypothesis testing, and one of the two well-differentiated
181 cells with high *CDX2* levels (DLD1) as the negative control (**Figure 2A**). PF was capable of inducing cell
182 death within 48 h in *CDX2*-low HCT116 and Sw480 cells but not the *CDX2*-high DLD1 cells (IC50's in 6-7
183 μM range vs > 40 μM, respectively; **Figure 2B**; **Figure S4A**). In both *CDX2*-low cell lines, PF-induced cell
184 death was preceded by induction of differentiation and suppression of stemness markers, at both transcript
185 (**Figure 2C**) and protein (**Figure S4B-E**) levels in a dose-dependent manner. These effects were associated
186 also with dose-dependent increase in apoptosis (**Figure S5A-H**). PF failed to reinstate *CDX2,* change other
187 markers of stemness and differentiation (**Figure 2D**) or induce cell death (**Figure 2E**) in *PRKAB1*-depleted
188 cells, thereby demonstrating that its anti-cancer action is target specific. Finally, Metformin which is a global,
189 non-specific and indirect agonist of all forms of the trimeric AMP-kinase (regardless of whether PRKAB1 or
190 PRKAB2 is the β-subunit within the αβγ trimer) failed to trigger cell death or induce *CDX2* expression even
191 at very high doses (**Figure 2B**; **Figure S5I-K**), suggesting that PRKAB1-specific effect is required for
192 therapeutic potency.

193 When implanted subcutaneously as xenografts in nude mice (**Figure 2F**), HCT116 tumors revealed
194 a 68% reduction in tumor volume (total AUC for vehicle and PF time series were 51280.23 and 26676.77,
195 respectively; **Figure 2G-I**) and an ~62.48% increase in survival (**Figure 2J**; Mantel-Haenszel Hazard Ratio
196 of 0.09 for reduction in death rates). PF promoted glandular structures within tumor (see legend **Figure S6A**),
197 reinstated *CDX2*, induced differentiation markers and suppressed stemness markers, as determined by
198 qPCR (**Figure 2K**). Reinstatement of CDX2 protein and its nuclear localization, alongside upregulation of
199 PRKAB1 protein were confirmed also by immunohistochemistry (IHC; **Figure 2L-M; Figure S6B**). Consistent
200 with the notion that colon stem cells divide very slowly [80], PF triggered a ~3-fold increase in mitotic bodies
201 (**Figure S6C**; **Figure 2M**). Conventional markers of tumor differentiation were also observed, such as a
202 reduction of nuclear β-Catenin (**Figure S6D**; **Figure 2M**) with concomitant increase in junctional β-Catenin,
203 where it co-localized with E-Cadherin (**Figure 2N**; **Figure S6E**).
204

205 ***Target validation in patient-derived organoids***

206 We next assessed the impact of PF on 23 CRC PDOs (recruited as two prospective independent cohorts)
207 and 3 healthy colon PDOs (see **Table** and *Methods*; **Figure 3A**). The anti-cancer action (as determined by
208 low IC50 values) was limited only to *CDX2*-low CRC PDOs, whereas the drug was virtually inert (with IC50>40
209 μM) against *CDX2*-high PDOs as well as healthy colon PDOs (**Figure 3B**). Both *CDX2* ('seed' gene in the
210 network) and *PRKAB1* (network-derived therapeutic target) showed significant positive correlations with IC50
211 (**Figure 3B**). By contrast, *CCDC88A* (a network-derived stemness marker; see **Figure S1D**), showed a
212 significant inverse correlation with IC50 (**Figure 3B**). Hierarchical unsupervised clustering performed using
213 just 3 network-derived genes (*CDX2*, *PRKAB1* and *CCDC88A*) perfectly classified sensitive from resistant
214 PDOs (**Figure 3C**). PF treatment enhanced differentiation and suppressed stemness (**Figure 3D**), as
215 observed in CRC cell lines (**Figure 2C**) and in xenografts (**Figure 2K**) previously, but these impacts were
216 restricted only to *CDX2*-low CRC PDOs. A multivariate analysis performed on the cohort of CRC PDOs (see
217 **Supplemental Information 3** for all variables included) showed that *CDX2*-status was the strongest variable

218 that determined IC50 (**Figure 3E**). In addition, two additional co-variates emerged: (i) histological grade and
219 *KRAS*^{mut} status, which indicates that PF was less likely to work on moderate/well-differentiated tumors that
220 tend to frequently harbor oncogenic *KRAS* mutations (**Figure 3E**; **Table**).
221 The relationship between CDX2-induction therapy and KRAS-status suggested that CDX2 may not
222 be prognostic among *KRAS*^{mut} group because its expression remains high (i.e., not lost). A univariate analysis
223 on a large cohort of CRCs with known driver mutations and patient outcome confirmed that *CDX2* was indeed
224 a determinant of outcome in tumors with *KRAS*^{WT} (**Figure 3F**-*left*), but not in those with *KRAS*^{mut} (**Figure 3F**-
225 *right*). These findings suggest that although relatively small, our PDO cohort is sufficiently diverse and
226 representative of the heterogeneity in the clinic to have revealed the interplay between *CDX2* and *KRAS*^{mut}.
227

228 ***Indicators of therapeutic efficacy and target cell specificity***
229 RNA seq on all 3 models– CRC cell lines, xenografts, and PDOs—confirmed that PRKAB1 agonism met 3
230 *a priori* formulated metrics of success: (i) *CDX2* was reinstated, which was the primary therapeutic goal
231 (bubble plots in **Figure 4A**-*top row*; **4B**; violin plots in **Figure S7A-C**), (ii) markers of crypt top enterocytes
232 and Goblet cells, which are established surrogate markers of differentiation in the colon crypt [51,81] were
233 induced (**Figure 4A**-*middle row*; **Figure S7D-F**), and (iii) the network was perturbed predictably, i.e., genes
234 in clusters #2 and #3 were induced (**Figure 4A**-*bottom row*; **Figure S7G-I**). Of note, all three metrics were
235 fulfilled selectively in *CDX2*-low CRC cell lines, xenografts and PDOs, but not in *CDX2*-high PDOs or in
236 healthy PDOs (**Figure 4A**-*columns #5 and #6*; **Figure S7C, S7F, S7I**).
237 A recent effort, using an innovative machine-learning algorithm extracted transcriptomic and
238 epigenetic feature sets derived from healthy (normal) stem cells and their differentiated progeny; the work
239 released novel gene signatures of oncogenic dedifferentiation[82]. Those signatures revealed that *CDX2*-
240 reinstatement therapy had no effect on normal stem cell-related genes in healthy and CRC PDOs (**Figure**
241 **4C**) but specifically reduced the expression of genes that impart cancer-related stemness (**Figure 4D**), those
242 that enable somatic cell reprogramming (i.e., the Yamanaka factors which have been implicated in the origin
243 of CSCs[83] (**Figure 4E**) and those that define CRC-specific CSCs (**Figure 4F**).
244 Taken together these findings show that *CDX2*-reinstatement therapy selectively downregulates
245 CSC-programs that are unique to *CDX2*-low tumors, thereby sparing normal stem cells in the healthy colon
246 tissue as well as *CDX2*-high tumor cells.
247

248 ***Potential for synergy with other therapeutic modalities***
249 Lack of CDX2 expression in Stage II-III CRCs has been previously shown to be associated with benefits from
250 adjuvant chemotherapy [52]; CDX2-positive tumors lack such benefit. We asked how therapeutic reinstatement
251 of CDX2 in *CDX2*-low tumors may impact response to chemotherapy. PF treatment consistently altered a
252 panel of patient-derived gene signatures across all models tested; it induced signatures of favourable
253 response and suppressed signatures of non-response to diverse chemotherapeutic agents (e.g., 5-FU,
254 Oxaliplatin, FOLFIRI) (**Figure 4G-i**). Consistent with these gene expression changes, PF showed synergy
255 with a panel of chemotherapeutic agents (see legend, **Figure 4H**).

256 Similar observations were made when we extended the analysis to include other treatment modalities;
257 PF consistently induced gene signatures of response to anti-EGFR (Cetuximab; **Figure 4G-ii**) and other
258 tyrosine kinase inhibitors (TKIs; **Figure 4G-iii**), with a few notable exceptions (Afatinib and Gefitinib; **Figure**
259 **4G-iii**). PF also induced gene signatures of response and suppressed signatures of non-response to
260 immunotherapy (**Figure 4G-iv**). The latter is consistent with the observation that PF also robustly induced a
261 consensus molecular subtype (cms)-1 in all three model systems tested (**Figure 4G-v**); the immune
262 landscape in cms1 subtype is known to favour response to immune checkpoint inhibitors[84].
263
264 ***A molecular signature of therapeutic response and selectivity***
265 To define the nature of the therapeutic response, we leveraged RNA seq data from all 3 models to conduct
266 an integrated differential expression analysis (see *Methods*). Briefly, differentially expressed genes (DEGs)
267 from two independent models (cell lines and xenografts; **Supplemental Information 4-5**) were further refined
268 on a third model, the CRC PDOs (**Figure 5A**). A set of 50 DEGs emerged; these genes were expressed in
269 *CDX2*-low CRC PDOs at levels significantly higher than healthy or *CDX2*-high CRC PDOs (**Figure 5B**;
270 **Figure S8A-B**). We used this 50-gene signature as a computational tool to track the changes along the
271 stemness→differentiation axis that occurs due to reinstatement of *CDX2* and found that PF suppressed these
272 genes (**Figure 5B**; see **Supplemental Information 6**) to levels seen in healthy PDOs and *CDX2*-high CRC
273 PDOs (**Figure S8A-B**).
274 This 50-gene signature was notable for the presence of several unique CSC-associated genes, such
275 as, *AGR2* [85], *ASCL2* [86,87], *ALDH3A1* [88], and *TM4SF1* [89,90], that were not parts of CSC signatures identified by
276 machine-learning (**Figure 4C-F**). The 50 genes were enriched for pathways that are known to augment CSC
277 survival [91-94], e.g., PTK6-dependent JAK/STAT signaling, numerous growth factor receptor and non-receptor
278 TK and the Hippo/YAP pathways and loss of TGFβ signaling (**Figure 5C**). The selective upregulation of these
279 pro-survival pathways in *CDX2*-low CRCs (but not healthy PDOs or *CDX2*-high CRCs) suggests that their
280 concomitant and catastrophic withdrawal in the setting of *CDX2* reinstatement could be the reason for the
281 observed target-cell selectivity.
282
283 ***Impact of CDX2 reinstatement therapy on survival***
284 To assess the impact of differentiation therapy on disease outcome, we analyzed the ability of the 50-gene
285 signature of therapeutic response to stratify relapse/disease-free survival (RFS/DFS) in diverse cohorts of
286 CRC patients. Compared to patients whose tumor had a high 50-gene score (like the untreated *CDX2*-low
287 PDOs), those with a low 50-gene score consistently had a better outcome across all datasets analyzed
288 (**Figure 5D, G-I**). The odds ratio (O.R) was ~2.0 (**Supplemental Information 7**-*tab #1*), implying that high
289 expression of the 50-gene signature carries a double risk of death/recurrence and that therapeutic
290 reinstatement of *CDX2* will reduce that risk by 50%. A univariate analysis revealed that the 50-gene signature
291 and *CDX2* were significant deterministic covariates of RFS (**Figure 5E**-*left*) but emerged as the better of the
292 two in *KRAS*^{WT} (**Figure 5E**-*middle*). The 50-gene score also outperformed *CDX2* as a prognostic indicator,
293 consistently across all cohorts tested (**Figure S8C-F**; **Supplemental Information 7**). These findings show
294 that the positive impact of CDX2 reinstatement is better represented in the 50-gene score (compared to
295 *CDX2* alone). Consistent with our observations earlier in the case of *CDX2* (**Figure 3E**), the 50-gene

296 signature was not a factor in *KRAS*^{mut} tumors (**Figure 5E**-*right*). These results provide objective evidence that
297 therapeutic suppression of the 50-gene signature is a desirable therapeutic goal that could translate to
298 improved survival.

Discussion

The major discovery we report here is a network-rationalized strategy to push differentiation of CRC stem cells by reinstating *CDX2* expression and define the cellular, molecular, and translational impact of such reinstatement. Much like immunotherapy acts by reinvigorating a physiologic response, we show that *CDX2*-reistatement acts by reinvigorating yet another physiologic program, that of differentiation. We identify and validate one target (PRKAB1) and confirm the utility of a first-in-class agent with proven safety (PF-06409577) to exert a target- and cell-type specific pro-differentiation and anti-tumor effect. *CDX2*-reinstatement therapy also fulfilled a set of rigorous and objective metrics of success that were formulated *a priori,* and its efficacy can be objectively tracked using a set of companion biomarkers (*CDX2* expression and a 50-gene signature of therapeutic response). Mechanistically, we show that *CDX2*-reinstatement is associated with the suppression of key stemness genes and numerous pro-survival pathways to which *CDX2*-low CRC stem cells (but not normal stem cells) may be uniquely addicted. Finally, we provide evidence that *CDX2*-reinstatement therapy is expected to synergize with most existing therapeutic modalities and translate to a reduction in death/relapse by ~50%.

Translational potential and key considerations: We advocate for the findings to be translated into clinical trials, prioritized as follows. The study pinpointed *CDX2*-low CRCs, and more specifically, those with a high 50-gene signature, as the optimal target group that will maximally benefit from this form of therapy. That *CDX2*-high tumors were found to be more differentiated and more likely to harbor mutant *KRAS* (but not *BRAF*) is consistent with the fact that *KRAS*^{mut} promotes hyperplasia and mucinous differentiation[95], but not stemness[96] and that loss of CDX2 (as determined by IHC) is positively associated with *BRAF* ^{mut}[97] but inversely associated with *KRAS*^{mut}[97]. This intriguing distinction could be attributed to cell-type specific roles of *KRAS*/*BRAF*^{mut} reported recently[98]. *KRAS*^{mut} status, however, does not appear to have any bearing on the determination of therapeutic candidacy because the two cell lines that were prioritized here based on low *CDX2* expression levels are also *KRAS*^{mut}, [HCT116 (1 mutant allele; G13D) and Sw480 (both alleles mutated; G12V)], and are sensitive to PF. These findings are consistent with a population-based study on metastatic CRCs (mCRCs; n = 796) that showed loss of CDX2 (as determined by IHC) defines a small subgroup of *KRAS*^{mut} cases (~9%) with a worse prognosis[97], and hence, could benefit from differentiation therapy. We conclude that *KRAS*^{mut} status is a confounding co-variate that is associated with the differentiation status of a tumor; however, it should not override low-CDX2 and/or high-50-gene signature in the determination of who may benefit from differentiation therapy.

Because loss of *CDX2* is an adverse prognostic factor in stage IV and stage III/*BRAF*^{mut} CRCs[71,99], these subgroups can be prioritized for *CDX2*-reinstatement therapy with PRKAB1 agonist as single agent or together with other modalities.

Although *CDX2* is prognostic in stage II(MSS)[52,65,69]and stage III CRCs[52,100], the use of *CDX2*-reinstatement therapy in these subgroups deserves additional considerations, and even caution. In stage III disease, adjuvant chemotherapy has been a standard of care since the 90's based on the Moertel trial[101]; however, many in this subgroup relapse despite chemotherapy (variable ~15-75% based on T-N substage[102]) and die of disease[103]. Because CDX2 expression is associated with increased expression of the multi-drug resistance gene, MDR1, which is implicated in the chemoresistance of *CDX2*-pos tumors[104,105], the use of

339 PRKAB1 agonist in combination with conventional chemotherapeutic agents must wait despite demonstrable
340 synergy in our studies. Considering these factors, PRKAB1 agonist as a single agent or with other modalities
341 can instead be prioritized for those with *CDX2*-low tumors who relapse and/or progress to metastatic disease.
342 This is feasible because CDX2 expression status in CRCs is not affected by metastasis or chemotherapy[106].
343 If those studies show benefit, PRKAB1 agonist as single agent could be considered as a first-line option for
344 patients with *CDX2*-low tumors. Because stage II/III early-onset CRC is a subgroup that show worse outcome
345 (poorer DFS) than its late-onset counterparts[107], and the *CDX2*-*PRKAB1* relationship is strongly conserved
346 in this subgroup (**Figure S2A**), we advocate the inclusion of this group in future studies considering PRKAB1
347 agonists in stage II/III CRCs.
348 Finally, because the degree of differentiation dictates the susceptibility to *BRAF*-mut-driven
349 tumorigenesis[108,109], early-stage patients with histopathologic criteria not qualifying for chemotherapy might
350 be reconsidered for *CDX2*-reinstatement therapy if their tumor has focal or global loss of CDX2 and
351 mutated *BRAF*.
352
353 *Expected impact on pre-neoplastic lesions of the colon:*
354 There is sufficient literature on how *CDX2*-loss (and hence reduced differentiation) is permissive to CRC
355 initiation, especially along the serrated pathway[108-110] and in the setting of inflammatory bowel disease-
356 associated CRCs[111-113]. A recent study using mosaic *CDX2*-/- mouse models showed that *CDX2* serves as a
357 tumor suppressor gene in a non–cell-autonomous manner; *CDX2*-/- metaplastic pre-cancerous cells could
358 induce tumorigenesis from neighbouring non-metaplastic cells without themselves becoming cancerous.
359 Focused studies on PDOs derived from such high-risk population are expected to reveal if PRKAB1 agonists
360 such as PF can serve as prophylactic therapy for those at highest risk of CRCs.
361
362 *Study limitations:*
363 How PRKAB1-agonism translates to *CDX2*-reinstatement and/or crypt differentiation were not studied. Future
364 efforts will assess whether aberrant methylation at the CDX2 promoter reported previously[114,115] is reversed
365 or if the loss of the highly specialized, junction-localized, tumor-suppressive stress-polarity signaling
366 pathway[76,77] is reinstated. Given the relatively small size of PDO cohorts, these results will need to be further
367 validated. We advocate for these findings to be confirmed within the framework of randomized clinical trials,
368 in conjunction with RNA sequencing studies.

369 ## Conclusions

370 Despite being at the forefront of biomedical research, therapies that can reprogram CSCs in carcinomas had
371 not emerged. We have addressed this unmet need using an network-based approach that differs from the
372 current practice in three fundamental ways: 1) Target identification and prediction modeling that is guided by
373 a Boolean implication network; 2) Target validation in network-rationalized animal models that most
374 accurately recapitulate the CSC-specific *CDX2*-low state; 3) Target validation in human preclinical organoid
375 models that have the potential to test target-biomarker pairing and thereby, personalize the choice of
376 therapies. The combined synergy of these approaches validates a first-in-class agent in tracking and killing
377 CSCs, while sparing normal stem cells. As for the impact of these findings, it is noteworthy that despite level
378 1 evidence showing the prognostic role of CDX2, its independent validation through numerous
379 studies[52,65,66,68-70,79,116,117], and a compelling pharmacoeconomic justification (i.e., cost $ 50 000 per QALY)
380 for a CDX2-stratified decision to offer chemotherapy[118], prospective trials demonstrating the superiority of a
381 CDX2-stratified decision has not emerged. Consequently, current guidelines do not recommend CDX2 be
382 used in prognostication in CRCs[119-123]. Our finding that CDX2 is a companion biomarker for differentiation
383 therapy with PF [a drug that has been deemed as clinically safe in Phase 1 on healthy volunteers
384 (NCT02286882) and can be immediately repurposed], provides a compelling impetus for setting up
385 prospective trials that can rigorously test both claims.

386 **Data availability statement**

387 All transcriptomic datasets generated in this work has been deposited at NCBI GEO [GSE237623, GSE237624,
388 GSE237625]. The data underlying all the figures and tables are available in the article and its online supplemental
389 materials.

390

391 **Acknowledgements**

392 We are grateful to the staffs of the UC San Diego HUMANOID™ Center of Research Excellence, for support
393 in the logistical support in conducting the studies on human PDOs. This work was supported by the National
394 Institutes for Health (NIH) grants UG3TR002968 and UH3 TR002968 (to P.G), R01-GM138385 (to DS), and
395 R01-CA238042, R01-CA100768 and R01-CA160911 (to P.G) and VA Merit awards 1 I01 BX003856-01A1
396 and 1 I01 BX004494-01 (M.B). S.S was supported in part by a American Association of Immunologists (AAI)
397 Intersect Fellowship Program for Computational Scientists and Immunologists. Other sources of support
398 include: R01-AI155696 (P.G and D.S), R01-AI141630 (P.G), and UG3TR003355 (D.S. and P.G), a Torey
399 Coast Foundation Award (P.G, D.S, M.B, J.Y), and by three Padres Pedal the Cause awards #PTC2017,
400 #PTC2021 and #PTC2022. D.S and P.G were also supported by the Leona M. and Harry B. Helmsley
401 Charitable Trust. Funders had no role in study design or conclusions.

402

403 **Author Contributions**

404 SS, DS and PG conceptualized the study; SS and PG designed and analysed all parts of the study; JA, KP,
405 EV and CT acquired, expanded, biobanked and conducted all experiments with patient-derived organoids;
406 VC conducted immunocytochemistry studies; CRE conducted qPCR studies and assisted SS, VC and PG
407 on key parts of the study; ST and DS built and validated the network model; SS and PG conducted all other
408 computational and bioinformatic analyses; SA and MB conducted the xenotransplantation studies; JRS and
409 JY synthesized the pharmacophore; MB, JY, DS and PG secured funding; SS and PG prepared all display
410 items; PG wrote the first draft of the manuscript; all authors edited and approved the final version.

411

412 **Conflicts of Interest Statement**: The authors have declared that no conflict of interest exists.

413 ## Figures and Legends:

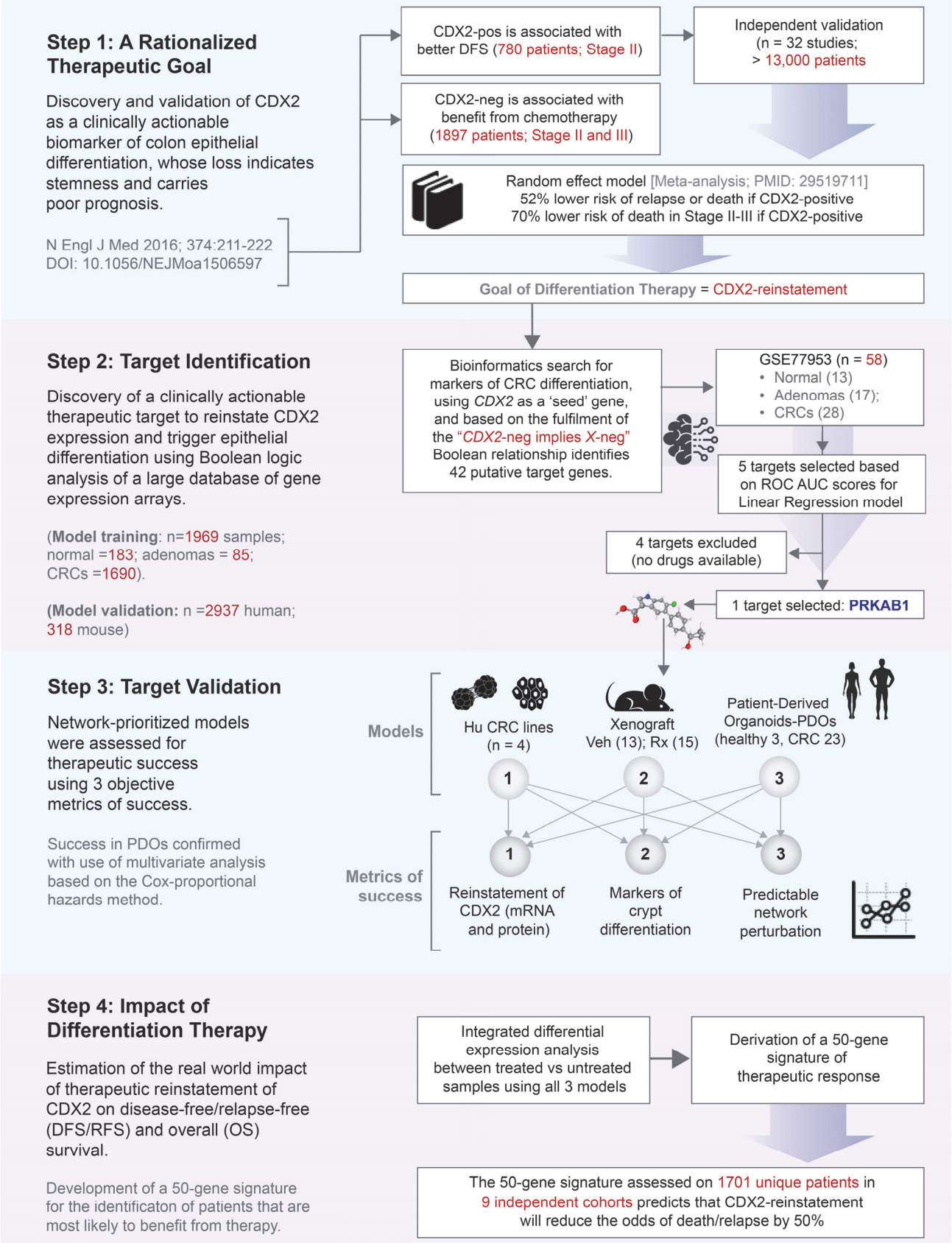

414

415 **Figure 1. Study Design: Identification and validation of a therapeutic strategy to reinstate CDX2**
416 **using ML.**

417 **Step 1**: Flow charts presents the emerging evidence, in chronological order, which rationalized reinstatement
418 of CDX2 as a desirable end goal for differentiating cancer stem cells in the most the aggressive subtypes of
419 CRCs.
420 **Step 2**. The key steps towards the network-based identification of PRKAB1 as a potent and actionable target,
421 whose agonism is predicted to reinstate CDX2 expression in those CRCs where its expression is lost.
422 **Supplemental Information 1** for a catalogue of all datasets used for model training and validation and
423 **Supplemental Information 2** for gene clusters, beyond *CDX2*, that are predicted to be co-induced upon
424 PRKAB1 agonism.
425 **Step 3.** Three model systems and objective metrics of success that are used to validate PRKAB1 agonism
426 as a strategy to reinstate CDX2 expression and induce differentiation.
427 **Step 4**. A 50-gene signature of therapeutic response derived from all 3 models is used to objectively measure
428 the impact of CDX2 reinstatement therapy and identify patients who are most likely to benefit from the same.

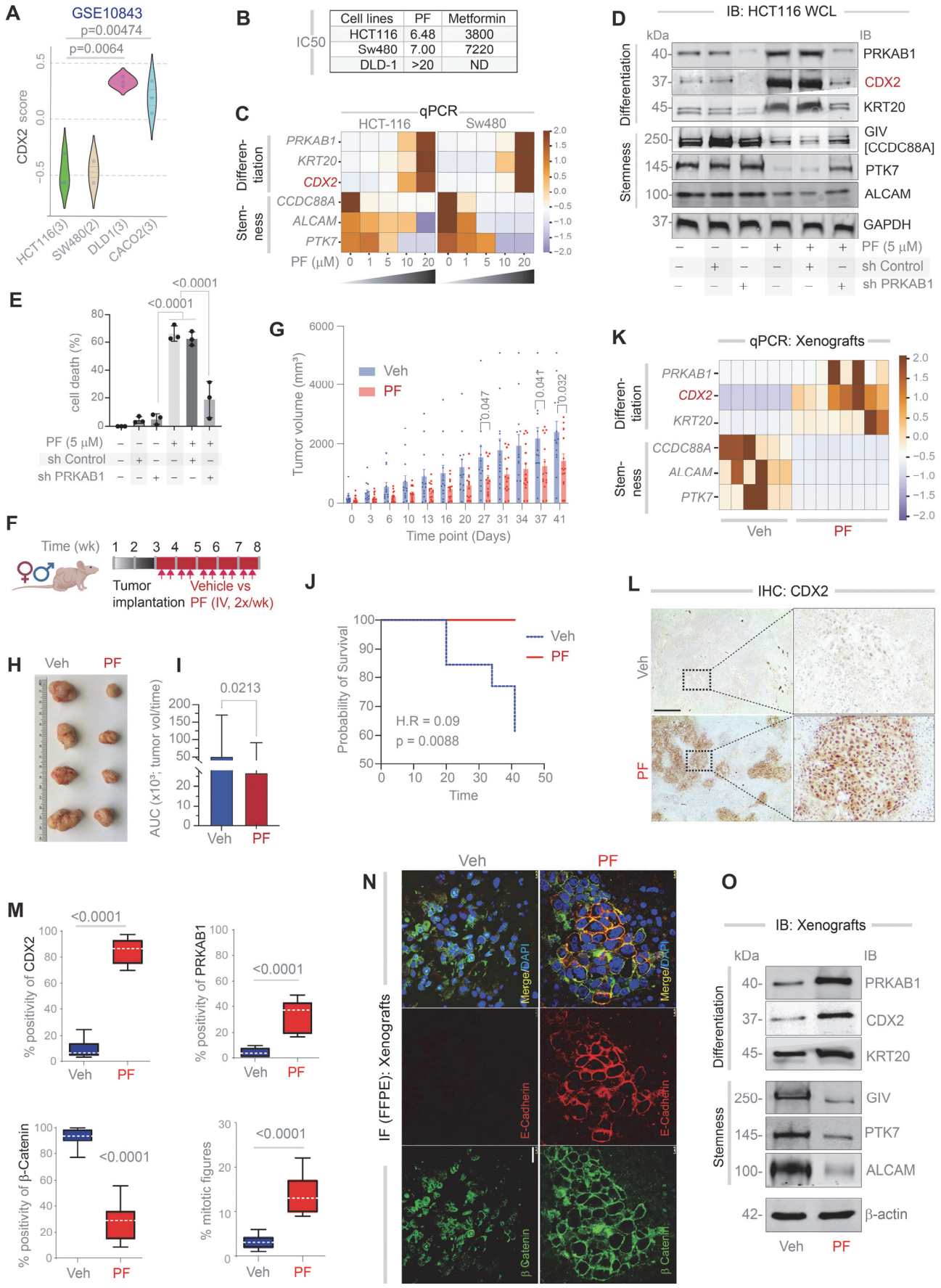

429

430 **Figure 2. Target validation in CRC cell lines and in xenotransplantation studies in mice. A**. Violin plot

431 displays *CDX2* expression (transcripts/million; tpm) in 4 common CRC cell lines. p-values are calculated

using Welch's t-test. **B**. Table shows IC50 values for specific (PF) or non-specific (Metformin) PRKAB1-agonists on CRC cell lines, as determined by MTT assays at 48 h. **C**. RT-qPCR on viable cells (>95%, at 16 h) of differentiation and stemness related markers in the colon is displayed as a heatmap of Z-score normalized values. **D-E**. Immunoblots (D) and MTT based survival assays (E) show the impact of PRKAB1 depletion (in HCT116 cells by shRNA) on the anti-cancer effect of PF. p-values are calculated using one-way ANOVA. Error bars indicate S.E.M of 3 independent biological experiments. See **Figure S4** and **S5** for additional studies on HCT116 and Sw480 cells challenged with increasing doses of PF (**S4** and **S5A-H**) or Metformin (**S5I-K**). **F**. Schematic showing experimental design and workflow. **G**. Graphs display growth kinetics of vehicle (Veh; n = 13) and PF-treated (n = 15) tumors, measured using callipers (2/wk), collated from 3 independent experimental cohorts. p-values are calculated using multiple paired t-test following Benjamini, Krieger, and Yekutieli method. **H**. Images of tumor xenografts at 8-wk post-implantation. **I**. Bar plots compare the area under the curve (AUC) of treatment and control arms [95% Confidence Interval was 31788.29 to 70772.18 (Veh) and 16949.29 to 36404.26 (PF); Error bars represent S.E.M., and p-value was determined by unpaired 2-tailed t-test using GraphPad]. **J**. Kaplan-Meier analysis shows time to the fulfilment of IACUC-mandated criteria for euthanasia (death and/or signs of discomfort). p-value was determined by Log Rank test. H.R., hazard ratio. **K**. RT-qPCR on xenografts displayed as a heatmap of Z-score normalized values. **L**. Representative fields from CDX2-stained FFPE-xenografts are shown. Scale bar = 100 μm. **M**. Quantification of CDX2, PRKAB1, and nuclear β-catenin staining by ImageJ (IHC profiler application) and mitotic bodies (manually counted in H&E-stained sections). p-values are calculated by unpaired 2-tailed t-test. See **Figure S6B-D** for images from representative fields. **N**. Representative fields from FFPE tumors co-stained for E-cadherin (red), β-catenin (green) and DAPI (nuclei; blue) are shown. Scale bar = 20 μm. See also **Figure S6K** for colocalization analysis by ImageJ. **O**. Immunoblots of lysates of viable tumor tissues. See **Figure S6F** for quantification.

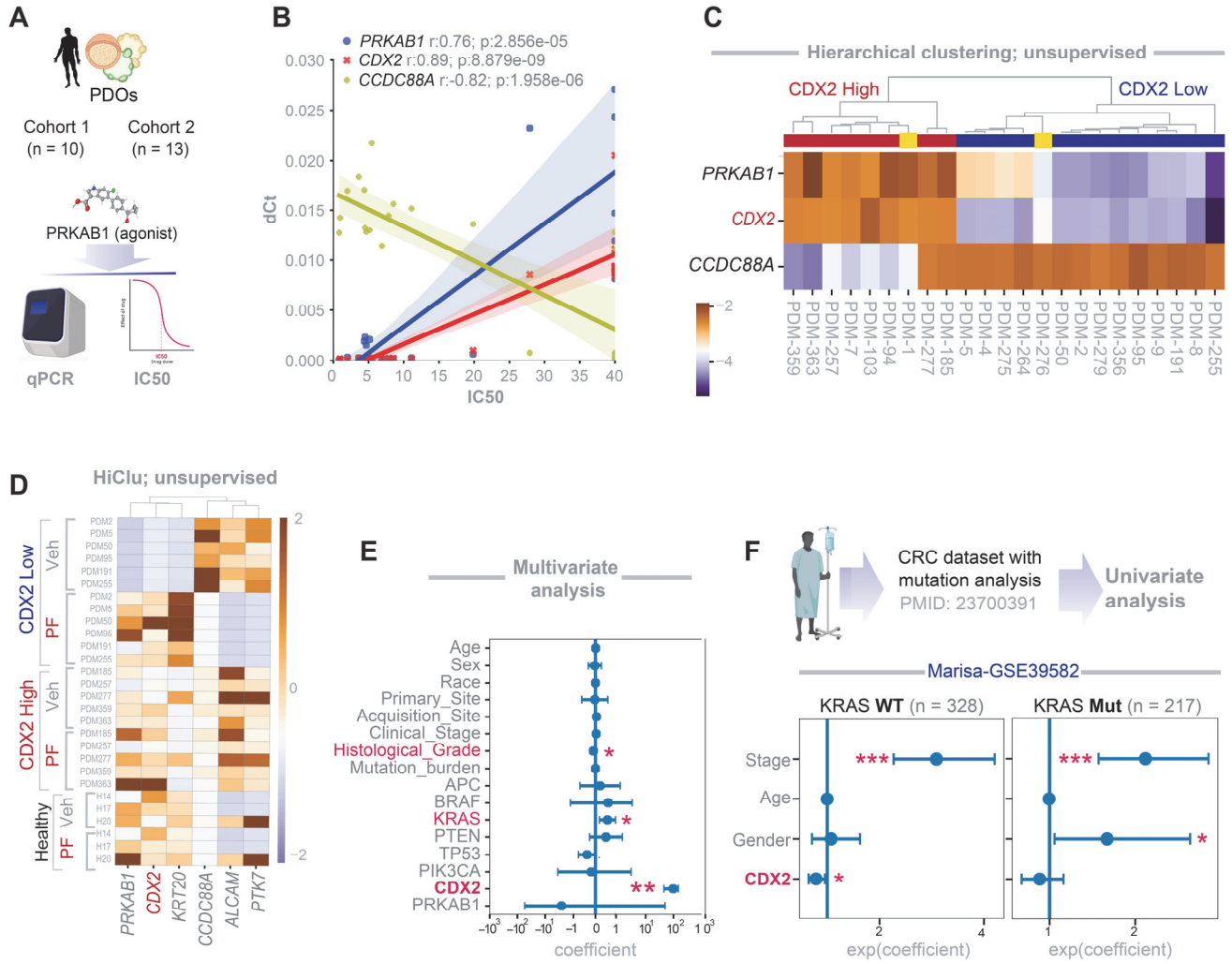

Figure 3. Differentiation and anti-cancer effects of PRKAB1 agonism are restricted to *CDX2*-low PDOs. A. Schematic of workflow for sequential analyses in two independent patient cohorts. See Supplemental Information 3 for patient demographics, tumor characteristics and mutation status of key genes. **B**. Correlation plots between IC50 and the levels of expression of 3 genes, as determined by qPCR. **C**. Heatmap displays the results of unsupervised clustering of the CRC PDOs using Z-score normalized qPCR estimation of 3 genes. **D**. Heatmap generated as above of the vehicle (Veh) and PF-treated CRC PDOs, using a panel of stemness and differentiation markers. **E**. Multivariate analysis of IC50 with PF as a linear combination of all variables in the PDOs used in this study. The coefficient of each variable (at the centre) with their upper and lower bounds of 95% confidence interval (as error bars) and the p-values from t-tests are illustrated in the bar plot. The p-value for each term tests the null hypothesis that the coefficient is equal to zero (no effect). Red = significant co-variates. *p ≤ 0.05; **p ≤ 0.01. See also Supplemental Information 3 for source data. **F**. Univariate analysis model of relapse-free survival (RFS) in KRAS-WT vs KRAS-mutant tumors in GSE39582. *p ≤ 0.05; **p ≤ 0.01; ***p ≤ 0.001.

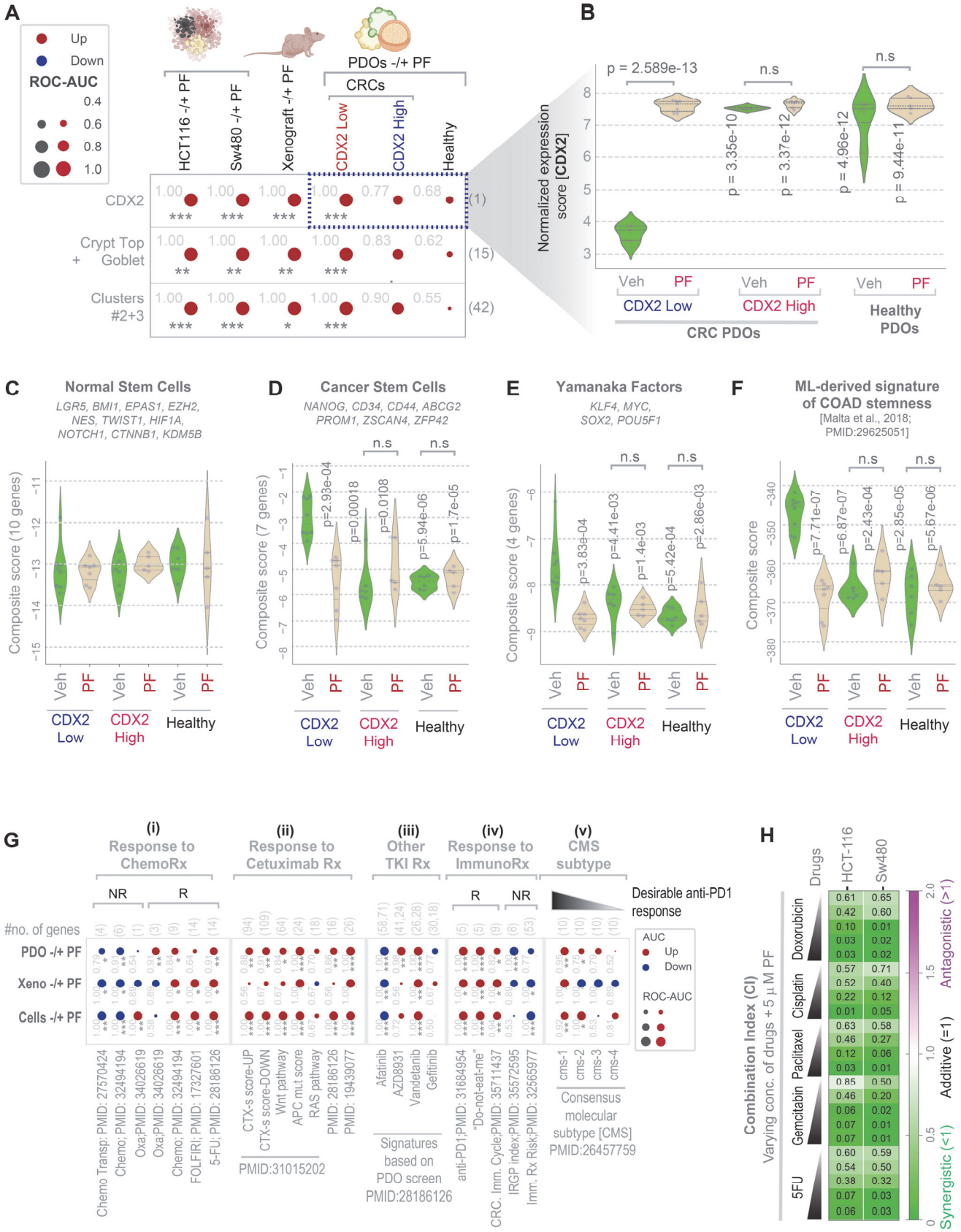

Figure 4. Indicators of success, target-cell specificity, and the potential for synergy with other treatment modalities. A. Expression of *CDX2* (top row), crypt top and Goblet cell markers (middle row) and genes in clusters #2-3 in the network (bottom row) gene/gene signatures in HCT116, Sw480, xenografts and PDOs is visualized as bubble plots of ROC-AUC values (radius of circles are based on the ROC-AUC) for

475 the classification of vehicle (Veh) vs PF-treated samples. Colors indicate the direction of gene regulation (Up,
476 red; Down, blue) in the treated samples. The significance of AUC is determined based on Welch's t-test and
477 displayed using standard codes (''p>0.1, '.'p<=0.1, *p<=0.05, **p<=0.01, ***p<=0.001) next to the ROC-AUC
478 values. See **Figure S7** for the display of the same data as violin plots with actual p-values. **B**. Violin plots
479 show *CDX2* expression in PDOs. p-values are based on Welch's t-test compared to vehicle (Veh)-treated
480 *CDX2*-low PDOs. **C-F.** Violin plots display the composite score of stemness markers recently reported in a
481 pan-cancer effort that used machine learning. p-values were determined by Welch's t-test, comparing each
482 sample against vehicle (Veh)-treated *CDX2*-low PDOs. **G**. Expression of gene signatures of response
483 (default or indicated with 'R') or non-response (N.R.) to multiple therapeutic modalities in CRC cell lines,
484 xenografts and PDO is visualized as bubble plots of ROC-AUC values (radius of circles are based on the
485 ROC-AUC) for the classification of vehicle (Veh) vs PF-treated samples. Colors indicate the direction of gene
486 regulation (Up, red; Down, blue). p-values displayed are based on significance of AUC using Welch's t-test
487 and using standard code (*p<=0.05, **p<=0.01, ***p<=0.001) next to the ROC-AUC. **H**. IC50 values for
488 combinations of 5 μM PF (constant) with increasing conc. of the indicated chemotherapeutic agents, as
489 determined on HCT116 and sw480 cell lines by MTT assays were used to derive a combination index (CI)
490 using a previously established formula [124]. Results are displayed as a heatmap.

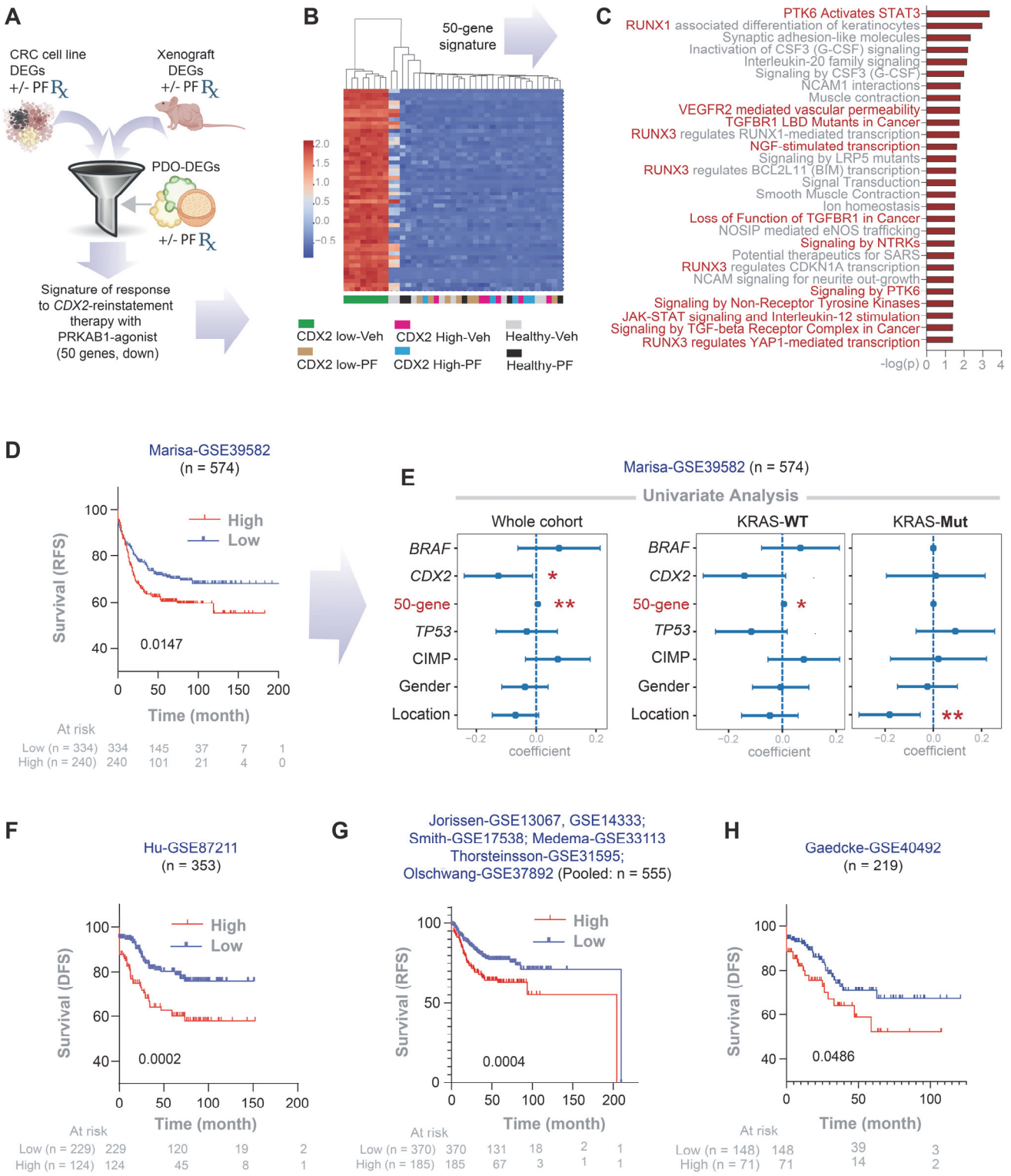

Figure 5. A gene signature for tracking therapeutic response and estimating impact on survival. **A**. Computational workflow used in the derivation of a 50-gene signature of therapeutic response using an integrated differential expression analysis (DEA) approach. Differentially expressed genes (DEGs) from CRC cell lines and xenografts (see **Supplemental Information 4-6**) were further refined based on their ability to accurately classify PDO samples with/without PF treatment (see **Supplemental Information 6** for gene list rank-ordered by ROC-AUC score). **B**. Heatmap displays the results of unsupervised clustering of PDOs

499 based on the 50-gene signature. Veh, vehicle. See **Figure S8A-B** for visualization of findings as violin plots.
500 **C**. Reactome pathway analysis of the 50-gene signature. **D**, **F-H**. Kaplan-Meier (KM) plots show recurrence-
501 free (RFS) or disease-free (DFS) survival over time on various cohorts of CRC patients, stratified by high vs
502 low expression scores of the 50-gene signature. p-values were determined by Log Rank test. See **Figure**
503 **S8C** for KM plots on the same cohorts based on *CDX2*-based stratification. **E**. Univariate analysis models of
504 RFS as a linear combination of all variables in a large CRC cohort, including the 50-gene signature. The
505 coefficient of each variable (at the centre) with 95% CI (as error bars) and the p values are illustrated. The p-
506 value for each term tests the null hypothesis that the coefficient is equal to zero (no effect). Left, entire cohort;
507 middle, *KRAS*-WT CRCs; right, *KRAS*-mut CRCs. *$p \leq 0.05$; **$p \leq 0.01$.

508 ## References

509 1. Stone RM, Maguire M, Goldberg MA, Antin JH, Rosenthal DS, Mayer RJ. Complete remission in
510 acute promyelocytic leukemia despite persistence of abnormal bone marrow promyelocytes during
511 induction therapy: experience in 34 patients. Blood 1988;71(3):690-6.
512 2. Kantarjian HM, Keating MJ, Walters RS, et al. Acute promyelocytic leukemia. M.D. Anderson
513 Hospital experience. Am J Med 1986;80(5):789-97.
514 3. Cunningham I, Gee TS, Reich LM, Kempin SJ, Naval AN, Clarkson BD. Acute promyelocytic
515 leukemia: treatment results during a decade at Memorial Hospital. Blood 1989;73(5):1116-22.
516 4. Tallman MS, Andersen JW, Schiffer CA, et al. All-trans-retinoic acid in acute promyelocytic
517 leukemia. N Engl J Med 1997;337(15):1021-8. DOI: 10.1056/NEJM199710093371501.
518 5. Tallman MS, Andersen JW, Schiffer CA, et al. All-trans retinoic acid in acute promyelocytic
519 leukemia: long-term outcome and prognostic factor analysis from the North American Intergroup
520 protocol. Blood 2002;100(13):4298-302. DOI: 10.1182/blood-2002-02-0632.
521 6. De Botton S, Dombret H, Sanz M, et al. Incidence, clinical features, and outcome of all trans-retinoic
522 acid syndrome in 413 cases of newly diagnosed acute promyelocytic leukemia. The European APL
523 Group. Blood 1998;92(8):2712-8.
524 7. Testi AM, Biondi A, Lo Coco F, et al. GIMEMA-AIEOPAIDA protocol for the treatment of newly
525 diagnosed acute promyelocytic leukemia (APL) in children. Blood 2005;106(2):447-53. DOI:
526 10.1182/blood-2004-05-1971.
527 8. Fenaux P, Chevret S, Guerci A, et al. Long-term follow-up confirms the benefit of all-trans retinoic
528 acid in acute promyelocytic leukemia. European APL group. Leukemia 2000;14(8):1371-7.
529 9. Sanz MA, Martin G, Rayon C, et al. A modified AIDA protocol with anthracycline-based
530 consolidation results in high antileukemic efficacy and reduced toxicity in newly diagnosed
531 PML/RARalpha-positive acute promyelocytic leukemia. PETHEMA group. Blood 1999;94(9):3015-
532 21.
533 10. Mandelli F, Diverio D, Avvisati G, et al. Molecular remission in PML/RAR alpha-positive acute
534 promyelocytic leukemia by combined all-trans retinoic acid and idarubicin (AIDA) therapy. Gruppo
535 Italiano-Malattie Ematologiche Maligne dell'Adulto and Associazione Italiana di Ematologia ed
536 Oncologia Pediatrica Cooperative Groups. Blood 1997;90(3):1014-21.
537 11. Bots M, Verbrugge I, Martin BP, et al. Differentiation therapy for the treatment of t(8;21) acute
538 myeloid leukemia using histone deacetylase inhibitors. Blood 2014;123(9):1341-52. DOI:
539 10.1182/blood-2013-03-488114.
540 12. Yen K, Travins J, Wang F, et al. AG-221, a First-in-Class Therapy Targeting Acute Myeloid
541 Leukemia Harboring Oncogenic IDH2 Mutations. Cancer Discov 2017;7(5):478-493. DOI:
542 10.1158/2159-8290.CD-16-1034.
543 13. Medema JP. Targeting the Colorectal Cancer Stem Cell. N Engl J Med 2017;377(9):888-890. (In
544 eng). DOI: 10.1056/NEJMcibr1706541.
545 14. Butte AJ, Kohane IS. Unsupervised knowledge discovery in medical databases using relevance
546 networks. Proc AMIA Symp 1999:711-5.
547 15. Shameer K, Readhead B, Dudley JT. Computational and experimental advances in drug
548 repositioning for accelerated therapeutic stratification. Curr Top Med Chem 2015;15(1):5-20.
549 16. Shen Y, Alvarez MJ, Bisikirska B, et al. Systematic, network-based characterization of therapeutic
550 target inhibitors. PLoS Comput Biol 2017;13(10):e1005599. DOI: 10.1371/journal.pcbi.1005599.
551 17. Margolin AA, Wang K, Lim WK, Kustagi M, Nemenman I, Califano A. Reverse engineering cellular
552 networks. Nat Protoc 2006;1(2):662-71. DOI: 10.1038/nprot.2006.106.
553 18. van Someren EP, Wessels LF, Backer E, Reinders MJ. Genetic network modeling.
554 Pharmacogenomics 2002;3(4):507-25. DOI: 10.1517/14622416.3.4.507.
555 19. Kusonmano K. Gene Expression Analysis Through Network Biology: Bioinformatics Approaches.
556 Adv Biochem Eng Biotechnol 2017;160:15-32. DOI: 10.1007/10_2016_44.
557 20. Allocco DJ, Kohane IS, Butte AJ. Quantifying the relationship between co-expression, co-regulation
558 and gene function. BMC Bioinformatics 2004;5:18. DOI: 10.1186/1471-2105-5-18.
559 21. Arkin A, Ross J. Statistical Construction of Chemical Reaction Mechanisms from Measured Time-
560 Series. The Journal of Physical Chemistry 1995;99(3):970-979. DOI: 10.1021/j100003a020.
561 22. Jordan IK, Marino-Ramirez L, Wolf YI, Koonin EV. Conservation and coevolution in the scale-free
562 human gene coexpression network. Mol Biol Evol 2004;21(11):2058-70. DOI:
563 10.1093/molbev/msh222.
564 23. Lee HK, Hsu AK, Sajdak J, Qin J, Pavlidis P. Coexpression analysis of human genes across many
565 microarray data sets. Genome Res 2004;14(6):1085-94. DOI: 10.1101/gr.1910904.

24. Tavazoie S, Hughes JD, Campbell MJ, Cho RJ, Church GM. Systematic determination of genetic network architecture. Nat Genet 1999;22(3):281-5. DOI: 10.1038/10343.
25. Butte AJ, Tamayo P, Slonim D, Golub TR, Kohane IS. Discovering functional relationships between RNA expression and chemotherapeutic susceptibility using relevance networks. Proc Natl Acad Sci U S A 2000;97(22):12182-6. DOI: 10.1073/pnas.220392197.
26. Paik S, Shak S, Tang G, et al. A multigene assay to predict recurrence of tamoxifen-treated, node-negative breast cancer. N Engl J Med 2004;351(27):2817-26. DOI: 10.1056/NEJMoa041588.
27. Witten DM, Tibshirani R. Survival analysis with high-dimensional covariates. Stat Methods Med Res 2010;19(1):29-51. DOI: 10.1177/0962280209105024.
28. Alizadeh AA, Eisen MB, Davis RE, et al. Distinct types of diffuse large B-cell lymphoma identified by gene expression profiling. Nature 2000;403(6769):503-11. DOI: 10.1038/35000501.
29. Zhao H, Ljungberg B, Grankvist K, Rasmuson T, Tibshirani R, Brooks JD. Gene expression profiling predicts survival in conventional renal cell carcinoma. PLoS Med 2006;3(1):e13. DOI: 10.1371/journal.pmed.0030013.
30. Sahoo D, Swanson L, Sayed IM, et al. Artificial intelligence guided discovery of a barrier-protective therapy in inflammatory bowel disease. Nat Commun 2021;12(1):4246. (In eng). DOI: 10.1038/s41467-021-24470-5.
31. Ghosh P, Sinha S, Katkar GD, et al. Machine learning identifies signatures of macrophage reactivity and tolerance that predict disease outcomes. EBioMedicine 2023;94:104719. (In eng). DOI: 10.1016/j.ebiom.2023.104719.
32. Sahoo D, Seita J, Bhattacharya D, et al. MiDReG: a method of mining developmentally regulated genes using Boolean implications. Proc Natl Acad Sci U S A 2010;107(13):5732-7. (In eng). DOI: 10.1073/pnas.0913635107.
33. Inlay MA, Bhattacharya D, Sahoo D, et al. Ly6d marks the earliest stage of B-cell specification and identifies the branchpoint between B-cell and T-cell development. Genes Dev 2009;23(20):2376-81. (In eng). DOI: 10.1101/gad.1836009.
34. Chen JY, Miyanishi M, Wang SK, et al. Hoxb5 marks long-term haematopoietic stem cells and reveals a homogenous perivascular niche. Nature 2016;530(7589):223-7. (In eng). DOI: 10.1038/nature16943.
35. Chan CK, Seo EY, Chen JY, et al. Identification and specification of the mouse skeletal stem cell. Cell 2015;160(1-2):285-98. (In eng). DOI: 10.1016/j.cell.2014.12.002.
36. Dimov IK, Lu R, Lee EP, et al. Discriminating cellular heterogeneity using microwell-based RNA cytometry. Nat Commun 2014;5:3451. (In eng). DOI: 10.1038/ncomms4451.
37. Chan CK, Lindau P, Jiang W, et al. Clonal precursor of bone, cartilage, and hematopoietic niche stromal cells. Proc Natl Acad Sci U S A 2013;110(31):12643-8. (In eng). DOI: 10.1073/pnas.1310212110.
38. Seita J, Sahoo D, Rossi DJ, et al. Gene Expression Commons: an open platform for absolute gene expression profiling. PLoS One 2012;7(7):e40321. (In eng). DOI: 10.1371/journal.pone.0040321.
39. Cheah MT, Chen JY, Sahoo D, et al. CD14-expressing cancer cells establish the inflammatory and proliferative tumor microenvironment in bladder cancer. Proc Natl Acad Sci U S A 2015;112(15):4725-30. (In eng). DOI: 10.1073/pnas.1424795112.
40. Volkmer JP, Sahoo D, Chin RK, et al. Three differentiation states risk-stratify bladder cancer into distinct subtypes. Proc Natl Acad Sci U S A 2012;109(6):2078-83. (In eng). DOI: 10.1073/pnas.1120605109.
41. Shin K, Lim A, Zhao C, et al. Hedgehog signaling restrains bladder cancer progression by eliciting stromal production of urothelial differentiation factors. Cancer Cell 2014;26(4):521-33. (In eng). DOI: 10.1016/j.ccell.2014.09.001.
42. Sin MLY, Mach KE, Sinha R, et al. Deep Sequencing of Urinary RNAs for Bladder Cancer Molecular Diagnostics. Clin Cancer Res 2017;23(14):3700-3710. (In eng). DOI: 10.1158/1078-0432.CCR-16-2610.
43. Sahoo D, Wei W, Auman H, et al. Boolean analysis identifies CD38 as a biomarker of aggressive localized prostate cancer. Oncotarget 2018;9(5):6550-6561. (In eng). DOI: 10.18632/oncotarget.23973.
44. Bhamre S, Sahoo D, Tibshirani R, Dill DL, Brooks JD. Temporal changes in gene expression induced by sulforaphane in human prostate cancer cells. Prostate 2009;69(2):181-90. (In eng). DOI: 10.1002/pros.20869.
45. Ghosh P, Campos VJ, Vo DT, et al. AI-assisted discovery of an ethnicity-influenced driver of cell transformation in esophageal and gastroesophageal junction adenocarcinomas. JCI Insight 2022;7(18) (In eng). DOI: 10.1172/jci.insight.161334.

46. Bonhomme C, Duluc I, Martin E, et al. The Cdx2 homeobox gene has a tumour suppressor function in the distal colon in addition to a homeotic role during gut development. Gut 2003;52(10):1465-1471.
47. Silberg DG, Swain GP, Suh ER, Traber PG. Cdx1 and cdx2 expression during intestinal development. Gastroenterology 2000;119(4):961-971.
48. Chawengsaksophak K, James R, Hammond V, Köntgen F, Beck F. Homeosis and intestinal tumours in Cdx2 mutant mice. Nature 1997;386(6620):84-87.
49. Hryniuk A, Grainger S, Savory JG, Lohnes D. Cdx1 and Cdx2 function as tumor suppressors. Journal of Biological Chemistry 2014;289(48):33343-33354.
50. Sahoo D, Dill DL, Gentles AJ, Tibshirani R, Plevritis SK. Boolean implication networks derived from large scale, whole genome microarray datasets. Genome biology 2008;9(10):R157. (In eng).
51. Dalerba P, Kalisky T, Sahoo D, et al. Single-cell dissection of transcriptional heterogeneity in human colon tumors. Nat Biotechnol 2011;29(12):1120-7. (In eng).
52. Dalerba P, Sahoo D, Paik S, et al. CDX2 as a prognostic biomarker in stage II and stage III colon cancer. New England Journal of Medicine 2016;374(3):211-222.
53. Levin TG, Powell AE, Davies PS, et al. Characterization of the intestinal cancer stem cell marker CD166 in the human and mouse gastrointestinal tract. Gastroenterology 2010;139(6):2072-2082 e5. DOI: 10.1053/j.gastro.2010.08.053.
54. Weichert W, Knosel T, Bellach J, Dietel M, Kristiansen G. ALCAM/CD166 is overexpressed in colorectal carcinoma and correlates with shortened patient survival. Journal of clinical pathology 2004;57(11):1160-4. (In eng).
55. Dalerba P, Dylla SJ, Park IK, et al. Phenotypic characterization of human colorectal cancer stem cells. Proc Natl Acad Sci U S A 2007;104(24):10158-63. (In eng).
56. Derangère V, Lecuelle J, Lepage C, et al. Combination of CDX2 H-score quantitative analysis with CD3 AI-guided analysis identifies patients with a good prognosis only in stage III colon cancer. Eur J Cancer 2022;172:221-230. (In eng). DOI: 10.1016/j.ejca.2022.05.040.
57. Bennedsen ALB, Cai L, Hasselager RP, et al. An exploration of immunohistochemistry-based prognostic markers in patients undergoing curative resections for colon cancer. BMC Cancer 2022;22(1):62. (In eng). DOI: 10.1186/s12885-022-09169-0.
58. Azcue P, Guerrero Setas D, Encío I, et al. A Novel Prognostic Biomarker Panel for Early-Stage Colon Carcinoma. Cancers (Basel) 2021;13(23) (In eng). DOI: 10.3390/cancers13235909.
59. den Uil SH, de Wit M, Slebos RJC, et al. Quantitative analysis of CDX2 protein expression improves its clinical utility as a prognostic biomarker in stage II and III colon cancer. Eur J Cancer 2021;144:91-100. (In eng). DOI: 10.1016/j.ejca.2020.10.029.
60. Tarazona N, Gimeno-Valiente F, Gambardella V, et al. Detection of postoperative plasma circulating tumour DNA and lack of CDX2 expression as markers of recurrence in patients with localised colon cancer. ESMO Open 2020;5(5):e000847. (In eng). DOI: 10.1136/esmoopen-2020-000847.
61. Hestetun KE, Aasebø K, Rosenlund NB, Müller Y, Dahl O, Myklebust MP. Mismatch repair phenotype determines the implications of tumor grade and CDX2 expression in stage II-III colon cancer. Mod Pathol 2021;34(1):161-170. (In eng). DOI: 10.1038/s41379-020-0634-9.
62. Asgari-Karchekani S, Karimian M, Mazoochi T, Taheri MA, Khamehchian T. CDX2 Protein Expression in Colorectal Cancer and ItsCorrelation with Clinical and Pathological Characteristics, Prognosis, and Survival Rate of Patients. J Gastrointest Cancer 2020;51(3):844-849. (In eng). DOI: 10.1007/s12029-019-00314-w.
63. Ma C, Olevian D, Miller C, et al. SATB2 and CDX2 are prognostic biomarkers in DNA mismatch repair protein deficient colon cancer. Mod Pathol 2019;32(8):1217-1231. (In eng). DOI: 10.1038/s41379-019-0265-1.
64. Ben-Aharon I, Goshen-Lago T, Sternschuss M, et al. Sidedness Matters: Surrogate Biomarkers Prognosticate Colorectal Cancer upon Anatomic Location. Oncologist 2019;24(8):e696-e701. (In eng). DOI: 10.1634/theoncologist.2018-0351.
65. Hansen TF, Kjær-Frifeldt S, Eriksen AC, et al. Prognostic impact of CDX2 in stage II colon cancer: results from two nationwide cohorts. British Journal of Cancer 2018;119(11):1367-1373.
66. Pilati C, Taieb J, Balogoun R, Marisa L, De Reyniès A, Laurent-Puig P. CDX2 prognostic value in stage II/III resected colon cancer is related to CMS classification. Annals of Oncology 2017;28(5):1032-1035.
67. Nolte S, Zlobec I, Lugli A, et al. Construction and analysis of tissue microarrays in the era of digital pathology: a pilot study targeting CDX1 and CDX2 in a colon cancer cohort of 612 patients. J Pathol Clin Res 2017;3(1):58-70. (In eng). DOI: 10.1002/cjp2.62.

683 68. Zhang BY, Jones JC, Briggler AM, et al. Lack of caudal-type homeobox transcription factor 2
684 expression as a prognostic biomarker in metastatic colorectal cancer. Clinical colorectal cancer
685 2017;16(2):124-128.
686 69. Tomasello G, Barni S, Turati L, et al. Association of CDX2 expression with survival in early
687 colorectal cancer: a systematic review and meta-analysis. Clinical colorectal cancer 2018;17(2):97-
688 103.
689 70. Sjoerd H, de Wit M, Slebos RJ, et al. Quantitative analysis of CDX2 protein expression improves its
690 clinical utility as a prognostic biomarker in stage II and III colon cancer. European Journal of Cancer
691 2021;144:91-100.
692 71. Bruun J, Sveen A, Barros R, et al. Prognostic, predictive, and pharmacogenomic assessments of
693 CDX 2 refine stratification of colorectal cancer. Molecular oncology 2018;12(9):1639-1655.
694 72. Baba Y, Nosho K, Shima K, et al. Relationship of CDX2 loss with molecular features and prognosis
695 in colorectal cancer. Clinical cancer research 2009;15(14):4665-4673.
696 73. Olsen J, Eiholm S, Kirkeby L, et al. CDX2 downregulation is associated with poor differentiation and
697 MMR deficiency in colon cancer. Experimental and molecular pathology 2016;100(1):59-66.
698 74. Sahoo D, Dill DL, Tibshirani R, Plevritis SK. Extracting binary signals from microarray time-course
699 data. Nucleic Acids Res 2007;35(11):3705-12. DOI: 10.1093/nar/gkm284.
700 75. Ghosh P. The stress polarity pathway: AMPK 'GIV'-es protection against metabolic insults. Aging
701 (Albany NY) 2017;9(2):303-314. DOI: 10.18632/aging.101179.
702 76. Ghosh P, Swanson L, Sayed IM, et al. The stress polarity signaling (SPS) pathway serves as a
703 marker and a target in the leaky gut barrier: implications in aging and cancer. Life Sci Alliance
704 2020;3(3) (In eng). DOI: 10.26508/lsa.201900481.
705 77. Aznar N, Patel A, Rohena CC, et al. AMP-activated protein kinase fortifies epithelial tight junctions
706 during energetic stress via its effector GIV/Girdin. Elife 2016;5 (In eng). DOI: 10.7554/eLife.20795.
707 78. Gough NR. Maintaining Polarity in the Face of Energetic Stress. Science's STKE
708 2007;2007(386):tw166-tw166. DOI: doi:10.1126/stke.3862007tw166.
709 79. Graule J, Uth K, Fischer E, et al. CDX2 in colorectal cancer is an independent prognostic factor and
710 regulated by promoter methylation and histone deacetylation in tumors of the serrated pathway.
711 Clinical epigenetics 2018;10(1):1-12.
712 80. Boman BM, Huang E. Human colon cancer stem cells: a new paradigm in gastrointestinal oncology.
713 J Clin Oncol 2008;26(17):2828-38. (In eng). DOI: 10.1200/JCO.2008.17.6941.
714 81. Kalisky T, Rajendran PS, Sahoo D, et al. Analysis of human colon tissue cell composition using
715 single-cell gene-expression PCR. Journal of biomolecular techniques: JBT 2013;24(Suppl):S11.
716 82. Malta TM, Sokolov A, Gentles AJ, et al. Machine Learning Identifies Stemness Features Associated
717 with Oncogenic Dedifferentiation. Cell 2018;173(2):338-354 e15. DOI: 10.1016/j.cell.2018.03.034.
718 83. Friedmann-Morvinski D, Verma IM. Dedifferentiation and reprogramming: origins of cancer stem
719 cells. EMBO Rep 2014;15(3):244-53. (In eng). DOI: 10.1002/embr.201338254.
720 84. Guinney J, Dienstmann R, Wang X, et al. The consensus molecular subtypes of colorectal cancer.
721 Nat Med 2015;21(11):1350-6. (In eng). DOI: 10.1038/nm.3967.
722 85. Valladares-Ayerbes M, Blanco-Calvo M, Reboredo M, et al. Evaluation of the adenocarcinoma-
723 associated gene AGR2 and the intestinal stem cell marker LGR5 as biomarkers in colorectal
724 cancer. Int J Mol Sci 2012;13(4):4367-4387. (In eng). DOI: 10.3390/ijms13044367.
725 86. Li Y, Yuan Y, Yang L, et al. AT7867 Inhibits the Growth of Colorectal Cancer Stem-Like Cells and
726 Stemness by Regulating the Stem Cell Maintenance Factor Ascl2 and Akt Signaling. Stem Cells Int
727 2023;2023:4199052. (In eng). DOI: 10.1155/2023/4199052.
728 87. Jubb AM, Chalasani S, Frantz GD, et al. Achaete-scute like 2 (ascl2) is a target of Wnt signalling
729 and is upregulated in intestinal neoplasia. Oncogene 2006;25(24):3445-57. (In eng). DOI:
730 10.1038/sj.onc.1209382.
731 88. Durinikova E, Kozovska Z, Poturnajova M, et al. ALDH1A3 upregulation and spontaneous
732 metastasis formation is associated with acquired chemoresistance in colorectal cancer cells. BMC
733 Cancer 2018;18(1):848. (In eng). DOI: 10.1186/s12885-018-4758-y.
734 89. Chen G, She X, Yin Y, et al. Targeting TM4SF1 exhibits therapeutic potential via inhibition of cancer
735 stem cells. Signal Transduct Target Ther 2022;7(1):350. (In eng). DOI: 10.1038/s41392-022-01177-
736 7.
737 90. Tang Q, Chen J, Di Z, et al. TM4SF1 promotes EMT and cancer stemness via the Wnt/β-
738 catenin/SOX2 pathway in colorectal cancer. J Exp Clin Cancer Res 2020;39(1):232. (In eng). DOI:
739 10.1186/s13046-020-01690-z.
740 91. Matsui WH. Cancer stem cell signaling pathways. Medicine (Baltimore) 2016;95(1 Suppl 1):S8-S19.
741 DOI: 10.1097/MD.0000000000004765.

742 92. Yang L, Shi P, Zhao G, et al. Targeting cancer stem cell pathways for cancer therapy. Signal
743 Transduct Target Ther 2020;5(1):8. DOI: 10.1038/s41392-020-0110-5.
744 93. Gierut J, Zheng Y, Bie W, et al. Disruption of the mouse protein tyrosine kinase 6 gene prevents
745 STAT3 activation and confers resistance to azoxymethane. Gastroenterology 2011;141(4):1371-80,
746 1380.e1-2. (In eng). DOI: 10.1053/j.gastro.2011.06.071.
747 94. Liu C, Pan Z, Chen Q, et al. Pharmacological targeting PTK6 inhibits the JAK2/STAT3 sustained
748 stemness and reverses chemoresistance of colorectal cancer. J Exp Clin Cancer Res
749 2021;40(1):297. (In eng). DOI: 10.1186/s13046-021-02059-6.
750 95. Li X, Sun K, Liao X, Gao H, Zhu H, Xu R. Colorectal carcinomas with mucinous differentiation are
751 associated with high frequent mutation of KRAS or BRAF mutations, irrespective of quantity of
752 mucinous component. BMC Cancer 2020;20(1):400. DOI: 10.1186/s12885-020-06913-2.
753 96. Feng Y, Bommer GT, Zhao J, et al. Mutant KRAS promotes hyperplasia and alters differentiation in
754 the colon epithelium but does not expand the presumptive stem cell pool. Gastroenterology
755 2011;141(3):1003-1013 e1-10. DOI: 10.1053/j.gastro.2011.05.007.
756 97. Aasebø K, Dragomir A, Sundström M, et al. CDX2: A Prognostic Marker in Metastatic Colorectal
757 Cancer Defining a Better. Front Oncol 2020;10:8. (In eng). DOI: 10.3389/fonc.2020.00008.
758 98. Brandt R, Sell T, Luthen M, et al. Cell type-dependent differential activation of ERK by oncogenic
759 KRAS in colon cancer and intestinal epithelium. Nat Commun 2019;10(1):2919. DOI:
760 10.1038/s41467-019-10954-y.
761 99. Aasebø K, Dragomir A, Sundström M, et al. CDX2: a prognostic marker in metastatic colorectal
762 cancer defining a better BRAF mutated and a worse KRAS mutated subgroup. Frontiers in oncology
763 2020;10:8.
764 100. Slik K, Turkki R, Carpén O, et al. CDX2 loss with microsatellite stable phenotype predicts poor
765 clinical outcome in stage II colorectal carcinoma. The American journal of surgical pathology
766 2019;43(11):1473-1482.
767 101. Moertel CG, Fleming TR, Macdonald JS, et al. Levamisole and fluorouracil for adjuvant therapy of
768 resected colon carcinoma. New England Journal of Medicine 1990;322(6):352-358.
769 102. Sobrero AF, Puccini A, Shi Q, et al. A new prognostic and predictive tool for shared decision making
770 in stage III colon cancer. European Journal of Cancer 2020;138:182-188.
771 103. Taieb J, André T, Auclin E. Refining adjuvant therapy for non-metastatic colon cancer, new
772 standards and perspectives. Cancer Treatment Reviews 2019;75:1-11.
773 104. Delhorme J-B, Bersuder E, Terciolo C, et al. CDX2 controls genes involved in the metabolism of 5-
774 fluorouracil and is associated with reduced efficacy of chemotherapy in colorectal cancer.
775 Biomedicine & Pharmacotherapy 2022;147:112630.
776 105. Takakura Y, Hinoi T, Oue N, et al. CDX2 regulates multidrug resistance 1 gene expression in
777 malignant intestinal epithelium. Cancer research 2010;70(17):6767-6778.
778 106. Shigematsu Y, Inamura K, Mise Y, et al. CDX2 expression is concordant between primary colorectal
779 cancer lesions and corresponding liver metastases independent of chemotherapy: a single-center
780 retrospective study in Japan. Oncotarget 2018;9(24):17056.
781 107. Fontana E, Meyers J, Sobrero A, et al. Early-Onset Colorectal Adenocarcinoma in the IDEA
782 Database: Treatment Adherence, Toxicities, and Outcomes With 3 and 6 Months of Adjuvant
783 Fluoropyrimidine and Oxaliplatin. Journal of Clinical Oncology 2021;39(36):4009-4019.
784 108. Tong K, Pellón-Cárdenas O, Sirihorachai VR, et al. Degree of tissue differentiation dictates
785 susceptibility to BRAF-driven colorectal cancer. Cell reports 2017;21(13):3833-3845.
786 109. Sakamoto N, Feng Y, Stolfi C, et al. BRAFV600E cooperates with CDX2 inactivation to promote
787 serrated colorectal tumorigenesis. Elife 2017;6:e20331.
788 110. Felipe De Sousa EM, Wang X, Jansen M, et al. Poor-prognosis colon cancer is defined by a
789 molecularly distinct subtype and develops from serrated precursor lesions. Nature medicine
790 2013;19(5):614-618.
791 111. Coskun M. The role of CDX2 in inflammatory bowel disease. Danish medical journal
792 2014;61(3):B4820-B4820.
793 112. Coskun M, Olsen AK, Holm TL, et al. TNF-α-induced down-regulation of CDX2 suppresses MEP1A
794 expression in colitis. Biochimica et Biophysica Acta (BBA)-Molecular Basis of Disease
795 2012;1822(6):843-851.
796 113. Yin F, Xie H, Lai J, et al. Double negativity for expression of YAP1 and CDX2 defines an aggressive
797 type of colitis-associated cancer. Anticancer research 2020;40(10):5411-5416.
798 114. Kawai H, Tomii K, Toyooka S, et al. Promoter methylation downregulates CDX2 expression in
799 colorectal carcinomas. Oncology reports 2005;13(3):547-551.

115. Sun X, Yang Q, Rogers CJ, Du M, Zhu M-J. AMPK improves gut epithelial differentiation and barrier function via regulating Cdx2 expression. Cell Death & Differentiation 2017;24(5):819-831.
116. Bae JM, Lee TH, Cho N-Y, Kim T-Y, Kang GH. Loss of CDX2 expression is associated with poor prognosis in colorectal cancer patients. World journal of gastroenterology: WJG 2015;21(5):1457.
117. Reggiani Bonetti L, Lionti S, Vitarelli E, Barresi V. Prognostic significance of CDX2 immunoexpression in poorly differentiated clusters of colorectal carcinoma. Virchows Archiv 2017;471(6):731-741.
118. Alarid-Escudero F. CDX2 testing+ FOLFOX for CDX2-negative colon cancer patients cost-effective strategy. PharmacoEconomics & Outcomes News 2021;892:9-27.
119. Argilés G, Tabernero J, Labianca R, et al. Localised colon cancer: ESMO Clinical Practice Guidelines for diagnosis, treatment and follow-up. Annals of Oncology 2020;31(10):1291-1305.
120. Benson AB, Venook AP, Al-Hawary MM, et al. Colon cancer, version 2.2021, NCCN clinical practice guidelines in oncology. Journal of the National Comprehensive Cancer Network 2021;19(3):329-359.
121. Committee ACNCCGR. Guidelines for the prevention, early detection and management of colorectal cancer. Sydney: The Cancer Council Australia and Australian Cancer Network 2005.
122. Van Cutsem E, Cervantes A, Adam R, et al. ESMO consensus guidelines for the management of patients with metastatic colorectal cancer. Annals of Oncology 2016;27(8):1386-1422.
123. Baum M, Fallowfield L, Farewell V, Macbeth F, Treasure T. NICEGuidelines: management of colorectal cancer metastases. British Journal of Surgery 2020;107(9):e357-e357.
124. Foucquier J, Guedj M. Analysis of drug combinations: current methodological landscape. Pharmacol Res Perspect 2015;3(3):e00149. (In eng). DOI: 10.1002/prp2.149.